Available online at www.sciencedirect.com
SCIENCE DIRECT®
Journal of Catalysis 220 (2003) 226–232
JOURNAL OF CATALYSIS
www.elsevier.com/locate/jcat

Highly dispersed zinc oxide species on silica as active sites for photoepoxidation of propene by molecular oxygen

Hisao Yoshida,* Takashi Shimizu, Chizu Murata, and Tadashi Hattori

Department of Applied Chemistry, Graduate School of Engineering, Nagoya University, Furo-cho, Chikusa-ku, Nagoya 464-8603, Japan

Received 27 February 2003; revised 23 June 2003; accepted 26 June 2003

Abstract

The activity of silica-supported zinc oxide containing from 0.01 to 5 mol% of Zn was investigated in the photoepoxidation of propene by molecular oxygen at room temperature. With an increase in the Zn loading amount, the conversion of propene increased monotonically, while the yield of propene oxide (PO) increased up to 1 mol% of Zn and then decreased. The selectivity to PO was almost constant up to 0.1 mol% of Zn and then decreased. By means of XRD, UV-vis, and XANES/EXAFS spectroscopy, it was found that the highly dispersed (isolated) tetrahedral zinc oxide species were predominant in the ZnO/SiO_2 samples of low Zn loading amounts, while the aggregated species such as $[ZnO]_n$ clusters were dominant in the ZnO/SiO_2 samples of higher Zn loading. The former species were found to be responsible for the photoepoxidation of propene.

1. Introduction

Propene oxide (PO) is an important chemical intermediate for industry. Although the direct epoxidation of propene by molecular oxygen is the most desirable, only indirect processes of propene epoxidation have been industrially employed [1]. The development of heterogeneous catalytic systems for this reaction is still required. Recently, several systems have been reported for the direct epoxidation of propene by only molecular oxygen, for example, heterogeneous catalytic systems employing modified Ag catalysts [1–3], metal nitrate-modified Ti-MCM catalysts [4], zeolite-supported TiO_2 catalysts [5] and NaCl-modified $VCe_{1-x}Cu_x$ oxide catalysts [6], in addition to noncatalytic radical reaction systems [7,8].

Photocatalysis is one possible system for selective oxidation [9]. As for the photoepoxidation of propene, several systems have been reported [10–16]. Among the metal oxides of semiconductors, TiO_2 was found to be most active [10]. However, the selectivity to PO was still low; the main product was CO_2. In other systems such as Ba-Y-type zeolites [11–13], Nb_2O_5/SiO_2 [14], MgO/SiO_2, and SiO_2 [15,16], selectivity to PO was relatively high, but the activity was quite low. From these reports, however, the importance of the silica surface or silica matrix for design of photoepoxidation catalysts is implied. Thus, we examined 50 kinds of silica-supported samples and revealed some potentially interesting systems [17]. Furthermore, TiO_2/SiO_2 [17–19], TiO_2–SiO_2 [18–20], and CrO_x/SiO_2 [21] were found to promote the photoepoxidation of propene catalytically, and it was revealed that the isolated metal oxide species in these systems were effective for the photoepoxidation of propene.

The ZnO/SiO_2 system was found to be one of the best candidates for photocatalyzing this reaction [17,22], although bulk ZnO did not show such high PO selectivity [10,17,22]. This means that the dispersed zinc oxide species on silica would be suitable for photoepoxidation in contrast with bulk ZnO. However, the structure and properties of dispersed zinc oxide species have not been clarified yet. In the present study, we investigated the activity for the direct propene photoepoxidation and the structure of zinc oxide species on a series of ZnO/SiO_2 samples of various Zn loadings ranging from 0.01 to 30 mol%.

2. Experimental

2.1. Materials

Amorphous silica was prepared from $Si(OEt)_4$ by the sol-gel method followed by calcination in a flow of air

* Corresponding author.
E-mail address: yoshidah@apchem.nagoya-u.ac.jp (H. Yoshida).

0021-9517/$ – see front matter
doi:10.1016/S0021-9517(03)00292-6

at 773 K for 5 h [17]. Silica-supported zinc oxide samples, ZnO/SiO_2, were prepared by an impregnation method; calcined silica was impregnated by aqueous solutions of $Zn(NO_3)_2$, dried at 383 K for 12 h, and calcined at 773 K in a flow of air for 5 h [17,22]. The Zn content (mol%) was defined as N_{Zn} (mol)/(N_{Zn} (mol) + N_{Si} (mol)) × 100. A ZnO sample was commercially obtained (Kishida, 99.0%) and calcined in air at 773 K for 5 h.

2.2. Photoreaction test

Before each photoreaction test, the sample was heated in air up to 673 K and then evacuated. Subsequently, the sample was treated with 100 Torr of oxygen at 673 K for 1 h, followed by evacuation at 673 K for 1 h. The photooxidation of propene was carried out in a closed reaction vessel made of quartz (123.6 cm^3) for 2 h. The temperature of the catalyst bed was measured to be ca. 310 K, which was elevated from room temperature by photoirradiation. The reactants were propene (100 μmol, 15 Torr) and oxygen (200 μmol, 30 Torr). The catalyst (200 mg) was spread on the flat bottom (12.6 cm^2) of the vessel [23]. A 200 W Xe lamp was used as a light source. Products in the gas phase were analyzed by gas chromatography (GC-FID and GC-TCD). In addition, adsorbed products on the catalyst were collected by heating at 573 K, followed by GC analysis. The results presented here are the sum of each product yield.

2.3. Characterization methods

Specific BET surface area was calculated from the amount of N_2 adsorption at 77 K. Powder X-ray diffraction patterns were recorded on a Rigaku diffractometer RINT 1200 using Ni-filtered Cu-K_α radiation (40 kV, 20 mA). Diffuse reflectance UV-vis spectra were recorded at room temperature on a JASCO V-570 equipped with an integrating sphere covered with $BaSO_4$. Before recording a UV-vis spectrum, the sample was treated in the same manner as that before the photoreaction test, and transferred to the optical cell without exposure to the atmosphere by using a specially designed in situ cell.

Zn *K*-edge XAFS (XANES/EXAFS) spectra were measured on BL-7C [24] of the Photon Factory in High Energy Accelerator Research Organisation in Tsukuba (Japan), with a ring energy of 2.5 GeV and a stored current of 300–430 mA. The spectra were recorded at room temperature with a Si(111) double-crystal monochromator (d = 3.13551 Å). High-energy X-rays from high-order reflections were removed by tuning the double crystals to 60% of maximum intensity. The energy was defined by assigning the first shoulder of the Cu foil spectrum to 8980.3 eV. The spectrum of the ZnO/SiO_2 sample of high Zn loading (> 1.0 mol%) was recorded in transmission mode. For determination of incident X-ray intensity, an ionization chamber (17 cm) filled with N_2 (85%)–Ar (15%) was used, and for transmission X-ray an ionization chamber (31 cm) filled with N_2 (50%)–Ar (50%) was used. As for the sample of low Zn loading (< 1.0 mol%), the fluorescence mode was employed by using the Lytle detector for fluorescent X-rays [25], whose ionization chamber (30 mm) was filled with Ar (100%). It was confirmed that the 1.0 mol% ZnO/SiO_2 sample gave almost the same spectra in both transmission and fluorescence mode. The sample was treated in the same way as before the photoreaction test and then transferred into polyethylene packs in a dry N_2 atmosphere. Normalization of XANES and data reduction on EXAFS were carried out as described elsewhere [26].

3. Results and discussion

3.1. Photooxidation of propene

Table 1 shows the results of the photooxidation of propene by molecular oxygen on SiO_2, ZnO/SiO_2, and ZnO samples. The detected products were propene oxide, ethanal, propanal, acetone, acrolein, alcohols (methanol, ethanol, and propan-2-ol), hydrocarbons (ethene and butenes; HC), and CO_x (CO and CO_2). On the SiO_2 sample, propene conversion was low (0.76%), although PO was produced to some extent (18.7% selectivity, 0.14% yield). ZnO showed low conversion of propene (1.25%), which may be due to the low surface area of ZnO. More than a half of converted propene was completely oxidized into CO_x (51.9%), and the selectivity to PO was very low. The main product in partial oxidation was acetone (20.8%). It was therefore confirmed that ZnO has some photooxidation activity but it is not suitable for epoxidation [10,17,22].

On the other hand, all of the ZnO/SiO_2 samples showed higher PO yield than either SiO_2 or ZnO. As for the product distributions, the main product was PO over most of ZnO/SiO_2 samples. The complete oxidation to CO_x (6.2–12.5% selectivity) occurred much less than over ZnO. The photooxidation activity of the ZnO/SiO_2 samples varied with loading amount of Zn. The highest PO selectivity was 48.7% on the ZnO/SiO_2 sample containing 0.01 mol% of Zn, although propene conversion (0.47%) was low on this sample. The highest PO yield was obtained on the ZnO/SiO_2 sample containing 1.0 mol% of Zn.

Fig. 1 graphically depicts the variation of propene conversion and the yields of representative products with loading amounts of Zn. Among these ZnO/SiO_2 samples, the conversion of propene increased with increasing Zn content (Fig. 1a). The yield of PO increased up to 1.3% with increasing Zn loading up to an amount of 1 mol%, and then decreased (Fig. 1b). The yields of ethanal (Fig. 1c), propanal (Fig. 1d), and CO_x (Fig. 1e) increased monotonically with increasing Zn content.

Fig. 2 shows the product selectivity over the ZnO/SiO_2 samples. The samples having less than 0.1 mol% of Zn all showed high PO selectivity (Fig. 2a). The samples contain-

Table 1
Results on the photooxidation of propene on the SiO_2, ZnO/SiO_2, and ZnO samples

Zn content[a]	SA[b]	Propene conversion	PO[c] yield	Selectivity (%)							
(mol%)	($m^2\,g^{-1}$)	(%)	(%)	PO[c]	Ethanal	Propanal	Acetone	Acrolein	Alcohols	HC[c]	CO_x[c]
0[d]	670	0.76	0.14	18.7	11.0	5.6	10.0	13.8	0.0	33.1	7.8
0.01	672	0.47	0.23	48.7	14.4	4.0	12.6	3.2	0.0	8.3	8.9
0.05	610	1.3	0.57	45.3	13.8	7.6	11.8	5.8	1.0	8.6	6.2
0.1	607	1.9	0.87	45.3	16.7	8.8	11.3	4.7	1.2	5.7	6.2
0.2	683	2.3	0.83	35.8	15.4	14.4	13.2	5.6	1.4	7.2	6.9
1.0	613	4.8	1.3	27.1	16.8	17.2	11.6	5.9	3.6	7.5	10.3
5.0	682	6.7	1.1	16.7	18.0	20.5	13.6	5.6	5.5	7.5	12.5
100[e]	12	1.3	0.02	1.9	6.2	0.0	20.8	8.1	6.9	4.2	51.9

Catalyst, 200 mg; propene, 100 µmol; O_2, 200 µmol; the reaction time (irradiation time), 2 h.
[a] Zn content (mol%) was defined as N_{Zn} (mol)/(N_{Zn} (mol) + N_{Si} (mol)) × 100.
[b] BET specific surface area.
[c] PO stands for propene oxide; HC, hydrocarbons; CO_x, CO and CO_2.
[d] SiO_2.
[e] ZnO.

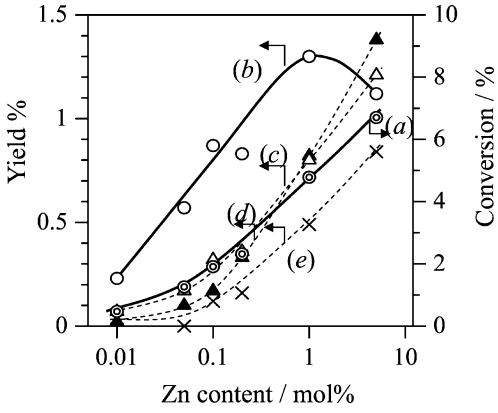

Fig. 1. Propene conversion (a) and product yield of propene oxide (b), ethanal (c), propanal (d), and CO_x (e) in the photooxidation of propene by molecular oxygen over ZnO/SiO_2 samples with varying Zn contents.

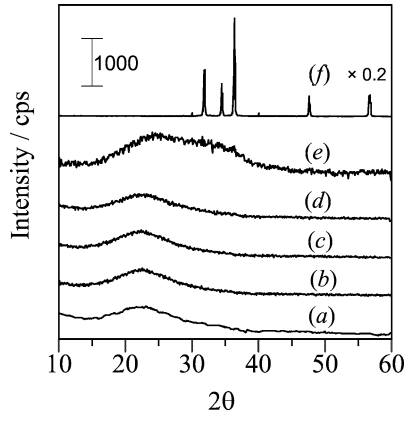

Fig. 3. X-ray diffraction patterns of the SiO_2 (a) and the ZnO/SiO_2 samples whose Zn contents were 0.1 (b), 1.0 (c), 5.0 (d), and 30 mol% (e) and that of pure ZnO (f).

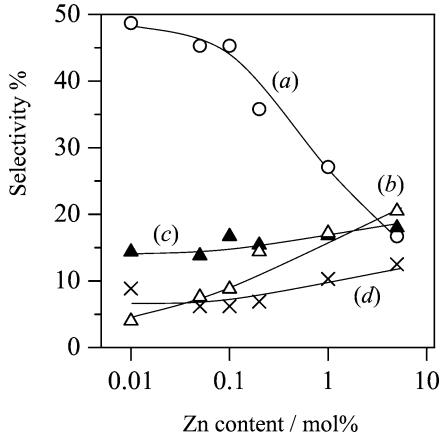

Fig. 2. Product selectivity for propene oxide (a), ethanal (b), propanal (c), and CO_x (d) in the photooxidation of propene by molecular oxygen over ZnO/SiO_2 samples with varying Zn content.

ing more than 0.1 mol% of Zn exhibited lower selectivity to PO; on these latter samples the selectivity to other products such as ethanal, propanal, and CO_x was relatively high (Fig. 2b–2d). In the separated reaction experiment on the ZnO/SiO_2 samples containing 0.05 and 5 mol% of Zn, almost the same PO selectivity (43 and 15%) at lower conversion (0.5 and 4.0%) was observed, respectively, implying that consecutive oxidation would not be a serious issue in this system. These results suggest that the variation of PO selectivity would mainly originate from the structure and electronic features of the active sites. Furthermore, highly dispersed zinc oxide species on the low Zn loading ZnO/SiO_2 samples seem to be suitable for PO formation in the photooxidation of propene by molecular oxygen.

3.2. The structure of ZnO/SiO_2 samples

For a better understanding of the structure of zinc oxide species, a ZnO/SiO_2 sample containing 30 mol% of Zn was additionally employed for the characterization study. Fig. 3 shows XRD patterns of the SiO_2, ZnO/SiO_2, and ZnO samples. The pure silica and ZnO/SiO_2 samples containing up to 5 mol% of Zn exhibited only very broad diffuse diffraction around 22° (Fig. 3a–3d). The 30 mol% ZnO/SiO_2 sample

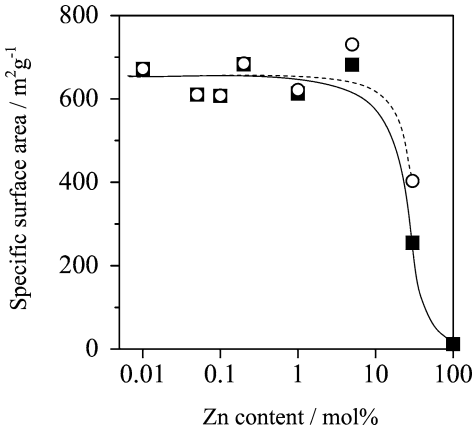

Fig. 4. Specific surface area (BET) of the ZnO/SiO_2 and ZnO samples. The closed square (solid line) shows the specific surface area per unit weight of the sample, while the open circles (broken line) shows the specific surface area per unit weight of SiO_2 support in the sample.

showed an additional very broad diffraction feature around 35° (Fig. 3e) which is possibly assignable to some kinds of zinc oxide species such as very small particles of ZnO.

Fig. 4 displays the variation of BET specific surface area of the ZnO and ZnO/SiO_2 samples with increasing Zn loadings. Both specific surface areas per unit weight of the ZnO/SiO_2 sample and per weight of SiO_2 support up to 5 mol% of Zn were almost the same as that of the pure silica (670 $m^2\ g^{-1}$). The 30 mol% ZnO/SiO_2 sample exhibited a very low value. These results suggest that the zinc oxide species on the samples of low Zn content were well dispersed on the silica surface without significantly changing the surface area of silica support. However, the zinc oxide species on the highest loading samples (e.g., 30 mol% Zn) would reduce the porosity of silica support.

3.3. The structure of the dispersed zinc oxide species on silica

Fig. 5 shows the diffuse reflectance UV-vis spectra of the samples, which reflect the electronic structure of photoabsorption sites. The pure silica exhibited a very small absorption band around at 240 nm (Fig. 6a, note that the scale is very small), which would be assignable to surface sites such as silanol and/or defect sites [27,28]. Bulk ZnO showed a large absorption band below the band gap at ca. 390 nm (Fig. 5h). The ZnO/SiO_2 samples (Fig. 5b–5g) showed different spectra from the bulk ZnO, meaning that the electronic structure of the Zn species on silica was completely different from that of Zn within bulk ZnO.

Both 0.05 and 0.1 mol% ZnO/SiO_2 samples exhibited a similar sharp absorption band around 200 nm along with a broad band at 240 nm that is due to silica surface sites (Fig. 5b and 5c). Since the sharp band around 200 nm became larger with increasing Zn loading, this band should be assigned to dispersed zinc oxide species on the silica surface.

With Zn content more than 0.2 mol%, the band intensity increased considerably, and the band edge was extended

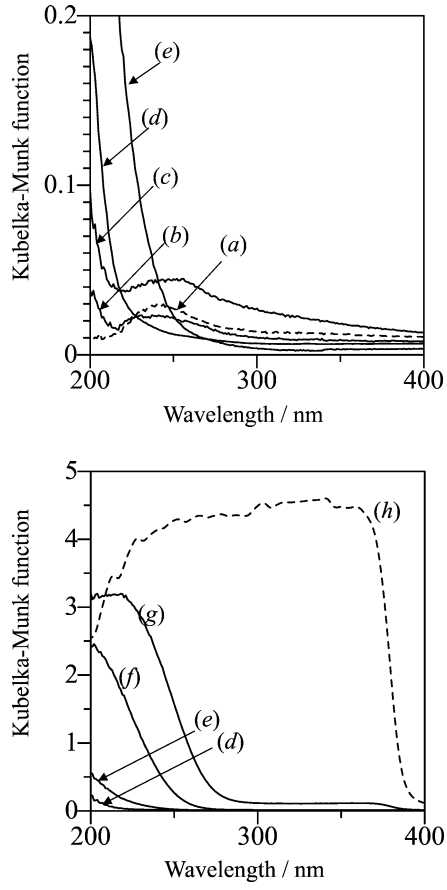

Fig. 5. Diffuse reflectance UV-vis spectra of SiO_2 (a) (broken line), the ZnO/SiO_2 samples whose Zn contents were 0.05 (b), 0.1 (c), 0.2 (d), 1.0 (e), 5.0 (f), and 30 mol% (g) and that of ZnO (h) (broken line). Spectra (d) and (e) are shown in both figures for the sake of comparison.

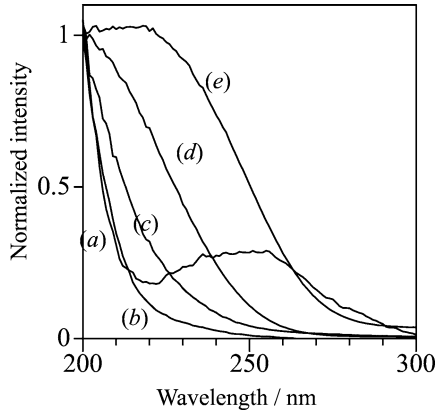

Fig. 6. Diffuse reflectance UV-vis spectra normalized by the intensity at 200 nm of the ZnO/SiO_2 samples whose Zn contents were 0.1 (a), 0.2 (b), 1.0 (c), 5.0 (d), and 30 mol% (e).

to a longer wavelength region (Fig. 5 d–5g). To clarify the variation of spectral line shape, the spectra were normalized at 200 nm and shown in Fig. 6. Both samples containing 0.1 and 0.2 mol% showed a similar spectral shape due to the dispersed zinc oxide species, except for the existence of the broad band centered around 250 nm on the 0.1 mol%

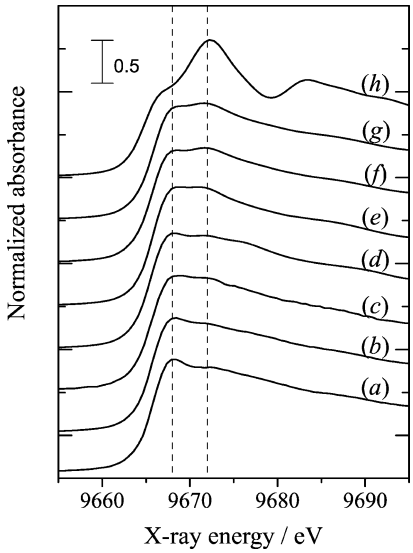

Fig. 7. Zn K-edge XANES spectra of the ZnO/SiO_2 samples whose Zn contents were 0.01 (a), 0.05 (b), 0.1 (c), 0.2 (d), 1.0 (e), 5.0 (f), and 30 mol% (g) and that of ZnO (h).

sample. The band due to zinc oxide species on the samples containing more than 0.2 mol% obviously varied in line shape with Zn loading amount. It is clear that the electronic structure of the zinc oxide species on the ZnO/SiO_2 samples depends on the loading of Zn; the low Zn loading ZnO/SiO_2 sample (< 0.2 mol% of Zn) has a distinguishable electronic structure from the others.

These variations of spectra with Zn content were similar to the case of TiO_2–SiO_2 systems [18,20,29–32], where it was realized that the highly dispersed (isolated) tetrahedral TiO_4 species exhibit a sharp absorption band below 250 nm due to ligand-to-metal charge transfer (LMCT) while the band is extended to a longer wavelength region as oligomers/clusters such as $[TiO_2]_n$ are formed. Analogous to this, it is proposed that the ZnO/SiO_2 samples with low Zn content (typically less than 0.2 mol%) would have highly dispersed zinc oxide species (possibly isolated), while the higher Zn content samples (typically more than 0.2 mol%) would have some aggregates such as oligomers/clusters species.

The band around 240 nm due to the silica surface vanished in the spectrum of the ZnO/SiO_2 sample containing 0.2 mol% of Zn (Fig. 5d). It was demonstrated that the dispersed zinc oxide species on the samples containing less than 0.2 mol% of Zn would be formed at the expense of the silica surface site. Since the photoabsorption sites on silica would probably be well scattered on the surface, it is expected that the formed zinc oxide species on the low loading samples (< 0.2 mol% of Zn) would be highly dispersed species (possibly isolated).

3.4. Local structure of zinc oxide species

X-ray absorption spectroscopy reveals the local structure of the target atom. XANES spectra generally reflect the coordination symmetry of the absorbing atom. Fig. 7 shows Zn K-edge XANES spectra of the ZnO/SiO_2 and ZnO samples. The main features of the XANES spectrum of ZnO (Fig. 7h) were a clear shoulder (9666 eV) around the absorption edge and the main peak (9672 eV) at the post edge. In bulk ZnO, the zinc atom is surrounded by 4 oxygen atoms in tetrahedral coordination as the $[ZnO_4]^{6-}$ unit [33]. There is no preedge peak due to $s-d$ transitions since the d-orbital of the Zn^{2+} cation is occupied.

The energy position of the absorption edge of XANES spectra of the ZnO/SiO_2 samples (Fig. 7a–7g) is the same as that of ZnO, indicating that the Zn was in an oxidized form and existed as a divalent cation. The spectral shape of XANES of the ZnO/SiO_2 samples was different from that of ZnO bulk, indicating that the local structure, especially the coordination symmetry, of zinc oxide species on silica is quite different from that in the bulk ZnO. The XANES spectra of the ZnO/SiO_2 samples were entirely featureless having only two broad maximums at 9668 and 9672 eV. The spectrum feature is quite similar to the reported Zn K-edge XANES of the Zn-containing glasses [34] and Zn-exchanged zeolite [35]. In addition to the fact that the Zn^{2+} cation in bulk ZnO is in the $[ZnO_4]^{6-}$ tetrahedral unit [33], it is known that the Zn cation is tetrahedrally coordinated by oxygen in crystalline Zn silicates where ZnO_4 tetrahedra link to surrounding silicate tetrahedra [34,36–38]. Thus, also in the present ZnO/SiO_2 system, it would be quite reasonable to expect that Zn exists as a divalent cation in a tetrahedral environment, ZnO_4 tetrahedra, on a silica surface. The spectral features of the ZnO/SiO_2 samples are quite similar to the reported Mg K-edge XANES of Mg oxide species dispersed on silica [15] and in zeolite [39]. This featureless shape of XANES might be typical of divalent cations tetrahedrally coordinated with oxygen without a d-orbital vacancy such as ZnO_4 and MgO_4 in/on silica or zeolites consisting of a SiO_2 tetrahedra network.

Comparing the spectra carefully, the relative intensity of the maximum at 9672 eV to that at 9668 eV increases slightly with an increase of Zn loading, suggesting that the local structure of zinc oxide species varied with Zn loading amount although the coordination symmetry remains tetrahedral. As noted above, the results from UV spectroscopy (Figs. 5 and 6) show that the ZnO/SiO_2 samples of low Zn content have predominantly highly dispersed (isolated) Zn species while the samples with high Zn content (> 0.2 mol% Zn) also have aggregates such as oligomers/clusters species. The slight increase of the relative intensity of the maximum at 9672 eV could be related to the increase of the second neighboring Zn atom, which might bring about slight distortions of the ZnO_4 tetrahedra, since the intensity increased with increasing Zn loading amount samples and was clearly observed as a main peak in the XANES of bulk ZnO. This interpretation is consistent with the results in the MgO/SiO_2 system [15].

Fig. 8 shows the k^3-weighted EXAFS oscillations of the ZnO/SiO_2 and ZnO samples. The difference between the

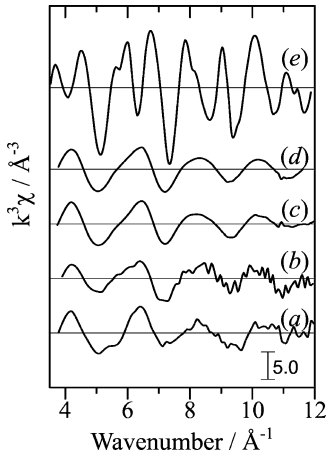

Fig. 8. k^3-weighted EXAFS spectra of the ZnO/SiO_2 samples whose Zn contents were 0.2 (a), 1.0 (b), 5.0 (c), and 30 mol% (d) and that of ZnO (e).

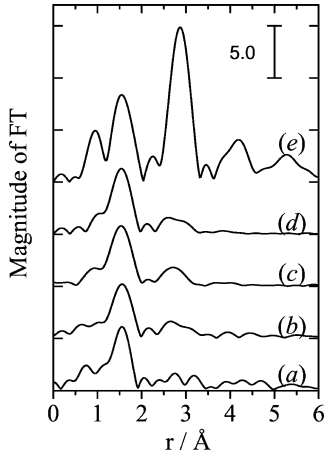

Fig. 9. Fourier-transformed EXAFS spectra of the ZnO/SiO_2 samples whose Zn contents were 0.2 (a), 1.0 (b), 5.0 (c), and 30 mol% (d) and that of ZnO (e).

ZnO/SiO_2 and ZnO samples is obvious. Supported zinc oxide species dispersed on silica have a different local structure from that in the bulk ZnO, such as distances to neighboring atoms in the first and second shells, and their coordination numbers. Unfortunately, the EXAFS of the 0.1 mol% ZnO/SiO_2 sample was too noisy to analyze. However, the EXAFS of even the 0.2 mol% ZnO/SiO_2 sample exhibited a small but obvious difference around 5.5–6 Å^{-1} from other ZnO/SiO_2 samples.

These EXAFS were Fourier-transformed as shown in Fig. 9. In the spectrum of ZnO, two distinct large peaks are observed around 1.5 and 2.9 Å; the former is assigned to the neighboring oxygen atoms in the first shell and the latter is due to the Zn atoms in the second shell. The spectra of the ZnO/SiO_2 samples showed a clear main peak at 1.5 Å, which is at the same position as bulk ZnO and similarly assignable to neighboring oxygen atoms. The peak intensity was also similar to that of bulk ZnO. These results indicate that the zinc oxide species on these samples have almost the same Zn–O bond length and coordination number as those in the bulk ZnO, i.e., ZnO_4 tetrahedra.

As for the second shell corresponding to a Zn–Zn distance around 2.5–3 Å, only small peaks were exhibited on ZnO/SiO_2 in comparison with bulk ZnO, indicating that the coordination number of neighboring Zn atoms would be very low in the ZnO/SiO_2 samples, or the of Zn–Zn distances would not be uniform. For the 30 mol% sample which exhibited very broad diffractions due to small ZnO crystallites (Fig. 3), there was only a small peak around 2.5–3 Å. This indicates that the ZnO crystallites would be in the minority, and other kinds of zinc oxide small aggregates such as oligomers/clusters would be in the majority. On the other hand, the 0.2 mol% sample showed no appreciable peaks around 2.5–3 Å, meaning that the major zinc oxide species would be highly dispersed (isolated) in very low Zn-loaded samples.

From the results derived from UV-vis spectra and XAFS (XANES/EXAFS) spectra, the structures of the zinc oxide species dispersed on the silica surface are suggested as follows: on low Zn content ZnO/SiO_2 samples (typically less than 0.2 mol%) the major zinc oxide species are atomically isolated tetrahedral ZnO_4 species, while in the higher content ZnO/SiO_2 samples (typically over 0.2 mol%) there are some kind of aggregated zinc oxide species such as oligomers/clusters consisting of ZnO_4 tetrahedra.

3.5. Active sites for the photoepoxidation of propene

From the results of the photooxidation tests, XRD, UV-vis, and XAFS spectroscopy noted above, it may be concluded that the active zinc oxide species showing high PO selectivity on the ZnO/SiO_2 samples are atomically isolated tetrahedral ZnO_4 species.

As shown in Table 1, silica itself also can produce PO. In this case, the active sites might be the special photoactive sites exhibiting the band around 240 nm in the UV spectrum (Fig. 5). By loading with Zn, these species are replaced with the isolated ZnO_4 species, and the PO selectivity increases further. This means that the isolated ZnO_4 species exhibit higher selectivity than the active sites of silica.

The PO selectivity on the 0.2 mol% ZnO/SiO_2 sample was a little lower than those on the samples containing less than 0.1 mol% of Zn, although the band due to zinc oxide species (less than 210 nm) seemed similar. However, XANES spectra varied slightly and continuously with variation of Zn loading. This indicates that some slight differences on the local structure of the dispersed zinc oxide species affect the PO selectivity. However, at this moment the possibility is not denied that the photoabsorption sites of the silica support that give rise to the broad band in Fig. 5 might also take part in the reaction.

On the other hand, the aggregated zinc oxide species, which is the majority species on the high loading ZnO/SiO_2 samples, would show low PO selectivity and produce also the other products such as ethanal, propanal, CO_x, and so

on. The difference on the electronic structure and the local structure between the aggregates and isolated species would influence the activity for the photooxidation of propene.

3.6. The role of the silica support

So far, several kinds of silica-based systems such as Nb_2O_5/SiO_2 [14,40], MgO/SiO_2 [15,16], TiO_2/SiO_2 [17–19], TiO_2–SiO_2 [18–20], and CrO_3/SiO_2 [21] have been reported to be active for the photoepoxidation of propene by molecular oxygen. Through these studies, it has become generally accepted that highly dispersed (isolated) tetrahedral metal oxide species on silica exhibit the highest selectivity in each system. One of the important roles of the silica matrix in these systems seems to be the isolation of the metal oxide species as tetrahedra species, thus creating the coordination sites for oxygen and propene.

It is well known that silica is an electrical insulator. When the M–O moiety in the isolated metal oxide species on the silica surface is photoexcited through charge transfer from oxygen to metal (ligand-to-metal charge transfer), the exciton (the electron–hole pair) can be localized on the metal–oxygen moiety. In the case of the TiO_2–SiO_2 system, it was confirmed that this localized hole on the lattice oxygen site of Ti–O moiety could activate the molecular oxygen to produce electrophilic O_3^- radical species that produce propene oxide [20]. On the contrary, the exciton is delocalized on the semiconductor photocatalysts such as TiO_2. It is also an important role of the silica to localize the exciton on the atomically dispersed metal oxide species; this localized exciton would promote the photoepoxidation.

4. Conclusion

In the present study, it was found that ZnO/SiO_2 with a low loading of Zn (< 0.1 mol% of Zn) exhibited high PO selectivity in the photooxidation of propene by molecular oxygen at room temperature. The active zinc oxide species responsible for the high PO selectivity are revealed to be the atomically highly dispersed (isolated) zinc oxide tetrahedral species on the silica surface.

Acknowledgments

The X-ray absorption experiment at the Zn K-edge was performed under the approval of the Photon Factory Program Advisory Committee (Proposal No. 99G253). This work was supported by a grant-in-aid from the Japanese Ministry of Education, Science, Art, Sports and Culture.

References

[1] J.R. Monnier, Appl. Catal. A 73 (2001) 221, and references therein.
[2] G. Lu, X. Zuo, Catal. Lett. 58 (1999) 67.
[3] J. Lu, M. Luo, H. Lei, C. Li, Appl. Catal. A 237 (2002) 11.
[4] T. Miyaji, P. Wu, T. Tatsumi, Catal. Today 71 (2001) 169.
[5] K. Murata, Y. Kiyozumi, Chem. Commun. (2001) 1356.
[6] J. Lu, M. Luo, H. Lei, X. Bao, C. Li, J. Catal. 211 (2002) 552.
[7] T. Hayashi, L.B. Han, S. Tsubota, M. Haruta, Ind. Eng. Chem. Res. 34 (1995) 2298.
[8] T.A. Nijhuis, S. Musch, M. Makkee, J.A. Moulijn, Appl. Catal. A 196 (2000) 217.
[9] A. Maldotti, A. Molinari, R. Amadelli, Chem. Rev. 102 (2002) 3811.
[10] P. Pichat, J. Herrmann, J. Disdier, M. Mozzanega, J. Phys. Chem. 83 (1979) 3122.
[11] F. Blatter, H. Sun, H. Frei, Catal. Lett. 35 (1995) 1.
[12] F. Blatter, H. Sun, S. Vasenkov, H. Frei, Catal. Today 41 (1998) 297.
[13] Y. Xiang, S.C. Larsen, V.H. Grassian, J. Am. Chem. Soc. 121 (1999) 5063.
[14] T. Tanaka, H. Nojima, H. Yoshida, H. Nakagawa, T. Funabiki, S. Yoshida, Catal. Today 16 (1993) 297.
[15] H. Yoshida, T. Tanaka, M. Yamamoto, T. Yoshida, T. Funabiki, S. Yoshida, J. Catal. 171 (1997) 351.
[16] H. Yoshida, T. Tanaka, M. Yamamoto, T. Funabiki, S. Yoshida, Chem. Commun. (1996) 2125.
[17] H. Yoshida, C. Murata, T. Hattori, J. Catal. 194 (2000) 364.
[18] C. Murata, H. Yoshida, T. Hattori, Stud. Surf. Sci. Catal. 143 (2002) 845.
[19] H. Yoshida, C. Murata, T. Hattori, Chem. Commun. (1999) 1551.
[20] C. Murata, H. Yoshida, J. Kumagai, T. Hattori, J. Phys. Chem. B 107 (2003) 4364.
[21] C. Murata, H. Yoshida, T. Hattori, Chem. Commun. (2001) 2412.
[22] H. Yoshida, C. Murata, T. Hattori, Chem. Lett. (1999) 901.
[23] H. Yoshida, M.G. Chaskar, Y. Kato, T. Hattori, J. Photochem. Photobiol. A 160 (2003) 47.
[24] M. Nomura, A. Koyama, M. Sakurai, KEK Rep. 91-1 (1991) 1.
[25] F.W. Lytle, R.B. Greegor, D.R. Sandstrom, E.C. Marques, J. Wong, C.L. Spiro, G.P. Huffman, F.E. Huggins, Nucl. Instrum. Methods 226 (1984) 542.
[26] T. Tanaka, H. Yamashita, R. Tsuchitani, T. Funabiki, S. Yoshida, J. Chem. Soc., Faraday Trans. 1 84 (1988) 2987.
[27] Y. Inaki, H. Yoshida, T. Hattori, J. Phys. Chem. B 104 (2000) 10304.
[28] Y. Inaki, H. Yoshida, T. Yoshida, T. Hattori, J. Phys. Chem. B 106 (2002) 9098.
[29] X. Gao, I.E. Wachs, Catal. Today 51 (1999) 233, and references therein.
[30] S. Bordiga, S. Colucia, C. Lamberti, L. Marchese, A. Zecchina, F. Boscherimi, F. Buffa, F. Genomi, G. Leofanti, G. Petrini, G. Vlaic, J. Phys. Chem. 98 (1994) 4125.
[31] L. Marchese, E. Gianotti, V. Dellarocca, T. Maschmeyer, F. Rey, S. Coluccia, J.M. Thomas, Phys. Chem. Chem. Phys. 1 (1999) 585.
[32] D.C.M. Dutoit, M. Schneider, R. Hutter, A. Baiker, J. Catal. 161 (1996) 651.
[33] R.G.W. Wyckoff, in: Crystal Structures, Vol. 1, Wiley, New York, 1963, p. 111.
[34] D.A. McKeown, I.S. Muller, A.C. Buechele, I.L. Pegg, J. Non-Cryst. Solids 261 (2000) 155.
[35] J.A. Biscardi, G.D. Meitzner, E. Iglesia, J. Catal. 179 (1998) 192.
[36] S.J. Louisnathan, Z. Kristallogr. 130 (1969) 427.
[37] C. Hang, M.A. Simonov, N.V. Belov, Sov. Phys. Crystallogr. 15 (1970) 387.
[38] R.J. Hill, G.V. Gibbs, J.R. Craig, Z. Kristallogr. 146 (1977) 241.
[39] H. Tsuji, F. Yagi, H. Hattori, H. Kita, in: L. Guczi, F. Solymosi, P. Tetenyi (Eds.), Proc. 10th Intern. Congr. Catalysis, Budapest, 1992, Vol. B, Akadémiai Liadó, Budapest, 1993, p. 1171.
[40] H. Yoshida, T. Tanaka, T. Yoshida, T. Funabiki, S. Yoshida, Catal. Today 28 (1996) 79.